Heat-Induced DNA Cleavage by Esperamicin Antitumor Antibiotics†

Yoshihiro Uesawa and Yukio Sugiura*
Institute for Chemical Research, Kyoto University, Uji, Kyoto 611, Japan
Received April 18, 1991; Revised Manuscript Received June 14, 1991

ABSTRACT: Esperamicin A_1 effectively breaks DNA strands upon heating at 50 °C. The preferential DNA cutting sites of heat-activated esperamicin A_1 are random and clearly differ from those of thiol- or UV-light-mediated DNA breakage with esperamicin A_1. The absence of heat-induced DNA cleavage by esperamicin Z and the induction of the DNA breakage by esperamicin A_1 disulfide indicate that (1) the enediyne core plays a significant role in this DNA strand scission and (2) the DNA cutting with the heat-activated esperamicin antibiotics does not necessarily require a trisulfide trigger in the aglycon portion. On the basis of the present results, a probable mechanism for the heat-induced DNA cleavage of esperamicin A_1 has been proposed.

Esperamicin, calicheamicin, neocarzinostatin, and dynemicin are unique antitumor antibiotics that mediate their DNA-damaging property and cytotoxicity primarily via oxidative strand scission (Golik et al., 1987; Lee et al., 1987; Goldberg, 1987; Sugiura et al., 1990). The antibiotics are characterized by the presence of an enediyne core. Esperamicin and calicheamicin also have a methyl trisulfide group that plays an important role as a trigger of the DNA cleavage reaction. Indeed, the cutting of DNA by esperamicin and calicheamicin antibiotics is greatly accelerated in the presence of thiol compounds (Long et al., 1989; Sugiura et al., 1989; Zein et al., 1988). Upon reduction with thiols, the methyl trisulfide group is cleaved and Michael addition of the resulting mercaptide ion to the bridgehead ene–one occurs followed by aromatization of the enediyne moiety via a 1,4-dehydrobenzene diradical. Recently, we have reported light-mediated DNA strand scission by esperamicin A_1 and dynemicin A (Uesawa et al., 1989; Shiraki & Sugiura, 1990). In these antibiotics, the observed nucleotide cleaving specificity is the same between the UV-light- and thiol-activated systems. In this paper, we report effective heat-induced DNA cleavage by esperamicin antibiotics, different nucleotide specificity of DNA strand scission by esperamicin A_1 in the heat and thiol systems, and a probable mechanism of the heat-mediated DNA cutting of esperamicin antibiotics.

Materials and Methods

Drugs and Chemicals. Esperamicins A_1, C, D, and Z were a generous gift of Dr. T. W. Doyle (Bristol-Myers Squibb). Esperamicin disulfide was prepared by treatment of esperamicin A_1 with methanethiol/acetonitrile according to the method for the preparation of calicheamicin disulfide (Ellestad et al., 1989) and identified by 400-MHz ^1H NMR spectra. The chemical structures of these esperamicin analogues are shown in Figure 1. Calicheamicin γ_1 was kindly supplied by Dr. G. A. Ellestad (American Cyanamid Comp.). *Sal*I and *Dra*II restriction endonucleases were obtained from Takara Shuzo (Kyoto, Japan). All other chemicals used were of commercial reagent grade.

DNA Cleavage Reaction. The reaction samples (total volume, 20 μL) contained 0.6 μg of pBR322 plasmid DNA, 1 mM deferoxamine, 10 mM EDTA, and 10 mM Tris-HCl buffer. Deferoxamine and EDTA were used to avoid the influence of contaminating metal ions such as iron and copper. The cleavage reactions were initiated by addition of esperamicins and carried out for 30 min in the dark. The reactions were stopped by the addition of cold ethanol (70 μL) and 3 mM sodium acetate. The samples were immediately chilled at −70 °C in a dry ice/ethanol bath. Each lyophilized sample was dissolved in 25 μL of loading buffer containing 0.05% bromophenol blue and 10% glycerol and heated at 90 °C for 1 min before electrophoresis. Electrophoresis was performed by using 1% agarose gel containing ethidium bromide (0.5 μg/mL). The amount of form I–form III DNAs in an agarose gel containing ethidium bromide was quantitated by scanning with a laser microdensitometer (LKB Model 2222 Ultro Scan XL).

Table I: Effect of Reaction Temperature on DNA Cleavage by Esperamicin A_1 (10 μM) at pH 9.5

reaction temp (°C)	amount of DNA (%)		
	form I	form II	form III
blank (intact DNA)	76.4	23.6	0.0
0	53.1	42.2	4.7
10	51.1	43.9	5.0
20	41.9	49.5	8.6
37	33.2	55.3	11.5
50	20.4	57.9	21.7
50 (−esperamicin)	75.5	24.5	0.0

Nucleotide Sequence Analysis. The reaction samples (total volume, 20 μL) contained the 5′-end-labeled 128-bp DNA fragment (pBR322, *Sal*I–*Dra*II), sonicated calf thymus DNA (225 μM base), 1 mM deferoxamine, 10 mM EDTA, and 20 mM Tris-HCl buffer (pH 7.5). The nucleotide sequence cleavages were initiated by addition of dithiothreitol (10 mM) at 20 °C or by incubation at 37 or 85 °C. Cold ethanol was added to the sample solutions in order to stop the reaction. Electrophoresis was performed in a 10% polyacrylamide/7 M urea slab gel at 2000 V for 90 min. DNA sequencing was carried out by the Maxam–Gilbert method (Maxam & Gilbert, 1980). The autoradiograms were scanned with the laser microdensitometer.

HPLC of Heated Esperamicin A_1. After heating at 65 °C for 18 h, the reaction product of esperamicin A_1 (1 mM) was separated by high-performance liquid chromatography (HPLC) on an A301-3S-120A ODS column (Yamamura Kagaku, Kyoto, Japan; 4.6 × 10 mm) with acetonitrile/0.1 M ammonium formate (pH 6.5) (50% v/v) as the solvent. The

† This study was supported in part by a Grant-in-Aid for Scientific Research on Priority Areas from the Ministry of Education, Science, and Culture of Japan.
* To whom correspondence should be addressed.

0006-2960/91/0430-9242$02.50/0

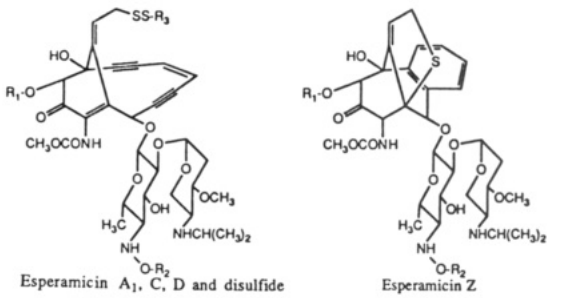

Functional gloups	Esperamicin analog A1	C	D	disulfide	Z
R_1	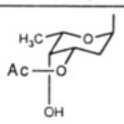	—H	—H	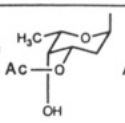	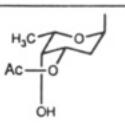
R_2	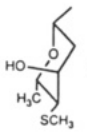	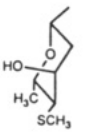	—H	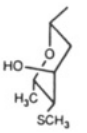	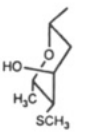
R_3	-S-CH_3	-S-CH_3	-S-CH_3	-CH_3	——

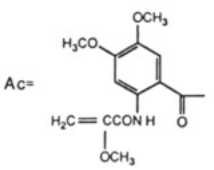

FIGURE 1: Structures of esperamicin analogues used in this study.

Table II: Effect of Esperamicin Concentration on DNA Strand Scission at 50 °C and pH 9.5

concn of esperamicin A_1 (μM)	amount of DNA (%) form I	form II	form III
blank (intact DNA)	76.4	23.6	0.0
100.0	0.0	45.1	54.9
10.0	20.4	57.9	21.7
1.0	55.2	38.3	6.5
0.1	67.8	29.5	2.7
0.0	75.5	24.5	0.0

eluate was monitored at 254 nm.

Results

Heat-Induced DNA Cleavage. Table I shows typical agarose gel electrophoretic results for heat-induced DNA strand scission by esperamicin A_1. In comparison to the DNA breakage at 20 and 37 °C, the antibiotic evidently stimulated DNA cleavage at 50 °C and converted covalently closed, supercoiled (form I) pBR322 DNA to nicked-circular (form II) and linear (form III) DNAs. The concentration dependency of the drug on the DNA strand scission at 50 °C is presented in Table II. In addition, Table III exhibits the effect of pH on the esperamicin-mediated DNA breakage at 50 °C. The result clearly indicates that the heat-induced DNA cleavage by esperamicin A_1 is stronger at pH 9.5 than at pH 7.5 or pH 6.5. In addition, similar thermally induced cleavage of DNA was also evidently observed in the other established enediyne-containing antibiotic such as calicheamicin γ_1 (see Table IV).

Heat-Induced DNA Cutting Activity of Esperamicin Analogues. Of special interest is the fact that esperamicin A_1 and its desulfido homologue gave similar heat-induced DNA cleavage activity (Figure 2). In the usual dithiothreitol-activation system, on the other hand, the DNA breakage ability of esperamicin A_1 disulfide was remarkably weaker than that of esperamicin A_1. Table IV compares the DNA cutting of esperamicins A_1, C, D, and Z and esperamicin A_1 disulfide at 50 °C. Esperamicin C also exhibited potent DNA breakage activity. In contrast, the activity of esperamicin D was much less and esperamicin Z showed no DNA cleavage activities.

Table III: Effect of pH on Heat-Induced (50 °C) DNA Cutting of Esperamicin A_1 (10 μM)

reaction pH	amount of DNA (%) form I	form II	form III
blank (intact DNA)	76.4	23.6	0.0
6.5	55.1	31.1	13.8
7.5	35.6	48.8	15.6
9.5	20.4	57.9	21.7

Table IV: Effect of Esperamicin Analogues (10 μM) on DNA Strand Scission at 50 °C and pH 9.5

esperamicin analogues	amount of DNA (%) form I	form II	form III
blank (without esperamicin)	75.5	24.5	0.0
esperamicin A_1	20.4	57.9	21.7
esperamicin C	31.1	27.1	41.8
esperamicin D	65.5	23.7	10.8
esperamicin Z	76.0	24.0	0.0
esperamicin disulfide	22.4	46.1	31.5
calicheamicin γ_1	0.0	12.9	87.1

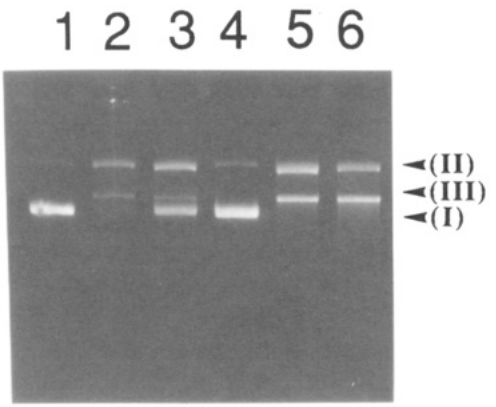

FIGURE 2: Agarose gel electrophoretic patterns of pBR322 DNA after treatment with 5 μM (lane 2) and 25 μM (lane 5) esperamicin A_1 or with 5 μM (lane 3) and 25 μM (lane 6) esperamicin A_1 disulfide. Lanes 1 and 4 show esperamicin-free samples. The reaction samples were incubated with 5 μM dithiothreitol (lanes 1–3) at 20 °C for 1 min or without dithiothreitol (lanes 4–6) at 50 °C for 30 min in the dark. Each sample solution was adjusted to pH 9.5.

Sequence Specificity of Heat-Induced DNA Cleavage by Esperamicin A_1. Cleavage data for the 5′-end-labeled DNA strand in the esperamicin A_1–heat system are presented in Figures 3 and 4. The same DNA fragment was treated with the esperamicin A_1–dithiothreitol system, and the DNA cutting sites were compared with the corresponding heat-induced DNA cleavage pattern. The thiol-activated esperamicin A_1 preferentially attacked at T and C bases in 5′-TT, 5′-CT, and 5′-CC sequences, whereas the cutting mode of heat-activated esperamicin A_1 was random as shown in the histograms. In thermally induced cleavage of DNA by esperamicin A_1, the sequence-specific pattern at 50 °C was almost the same as that at 37 °C. When dithiothreitol was used with esperamicin A_1 at 50 °C, the sequence-specific reaction took precedence over the thermal reaction.

HPLC Feature of Heated Esperamicin A_1. In the absence of DNA, HPLC analysis of the heat-activated esperamicin A_1

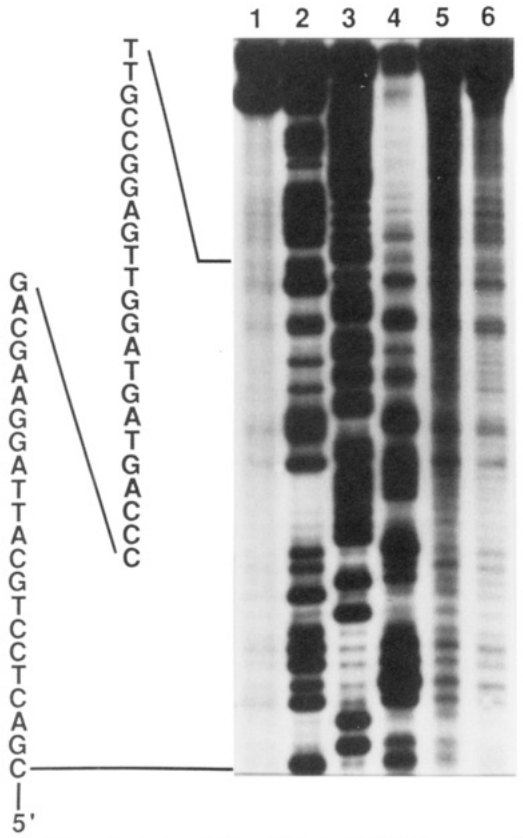

FIGURE 3: Strand scission of 5′-end-labeled DNA by esperamicin A_1 (0.2 μM) in the presence of dithiothreitol at 20 °C (lane 4) and by esperamicin A_1 (2 μM) at 85 °C (lane 5) and 37 °C (lane 6). Each sample solution was adjusted to pH 7.5 and was incubated for 15 min in the dark. Lanes 1, 2, and 3 show intact DNA and the Maxam–Gilbert sequencing reactions for C + T and A + G, respectively.

showed the formation of one major product (retention time 18.6 min). The same product was also obtained in the presence of calf thymus DNA, although its yield was somewhat lower than that in the absence of DNA. The reaction product is distinctly different from esperamicin Z (retention time 4.4 min), and its retention time reveals it to be a less polar compound than esperamicin A_1 (retention time 12.2 min). In addition, this compound was inactive for DNA cleavages by thiol, UV, and heat systems.

Discussion

We found that esperamicin A_1 shows potent DNA breakage activity at 50 °C, even in the absence of reducing agent and UV light radiation. Indeed, the antibiotic was irreversibly inactivated by preincubation at ≥50 °C. Esperamicin Z, in which the enediyne core was aromatized, showed no DNA cleavage activities under the same experimental condition. We prepared esperamicin A_1 disulfide to investigate whether the heat-induced DNA breakage activity is clearly related to its trisulfide-trigger site or not. As well as did esperamicin A_1, esperamicin A_1 disulfide strongly cut the super-coiled DNA at 50 °C. The result seems to indicate that the heat-induced DNA breakage of esperamicin antibiotics does not necessarily require the trisulfide trigger.

When dithiothreitol was used as an activation reagent of esperamicin A_1, this enediyne antibiotic showed the preferential cutting at T and C bases in oligopyrimidine sequences such as 5′-TTC, 5′-CTC, and 5′-TTT (Sugiura et al., 1989). The observed nucleotide cleavage specificity for the UV-light-activated esperamicin A_1 resembled that for the thiol-activated esperamicin A_1 (Uesawa et al., 1989). However, the present heat-induced nucleotide-sequence cleavage pattern of esperamicin A_1 is evidently different from the corresponding thiol- and light-induced DNA cutting modes. We suggested previously that (1) the fucoseanthranilate moiety does not contribute significantly to base recognition and (2) the enediyne moiety is the key functional group for sequence-specific cleavage in the esperamicin A_1–dithiothreitol system (Sugiura et al., 1989). Comparative experiments using esperamicins A_1, C, and D indicate that both the 2-deoxy-L-fucose and anthranilate aromatic ring moieties are not essential for the heat-induced DNA cleavage by esperamicin antibiotics. The thiomethyl hexapyranose moiety has an important effect on the heat-induced DNA cleavage activity of esperamicins. These results correspond well to those in the thiol-activated DNA strand scission by esperamicin antibiotics. In the thiol-activated DNA cleavages, the noted differences between esperamicin A_1 and its desulfido homologue may be due to a kinetic difference in the rate of mercaptide formation. Disulfides and trisulfides are expected to exhibit markedly different stabilities in the presence of reducing agents.

As proposed in the thiol-activated esperamicin A_1 and calicheamicin γ_1, the conversion of the enediyne core into the 1,4-dehydrobenzene diradical is the most important step for the DNA cutting activity of the drugs (Nicolaou et al., 1988a; Zein et al., 1989). The absence of DNA cleavage activity with esperamicin Z reveals that the enediyne portion plays an important role in the heat-induced cleavage of DNA by esperamicin A_1 and that a similar 1,4-dehydrobenzene diradical intermediate presumably participates in the present DNA strand scission. In addition, the potent heat-induced DNA cleavage activity of esperamicin A_1 disulfide suggests the presence of a trigger reaction other than the so-called trisulfide trigger. One reasonable mechanism for the diradical formation is direct rearrangement by thermal vibration of the enediyne moiety (Figure 5A). Such rearrangement of the enediyne that proceeds through the 1,4-dehydrobenzene diradical depends on the reaction temperature (Lockhart et al., 1981). The rearrangement product is also produced spontaneously as both ends of the triple bonds are closed by chemical modifications at room temperature (Nicolaou et al., 1988b; Snyder, 1989,

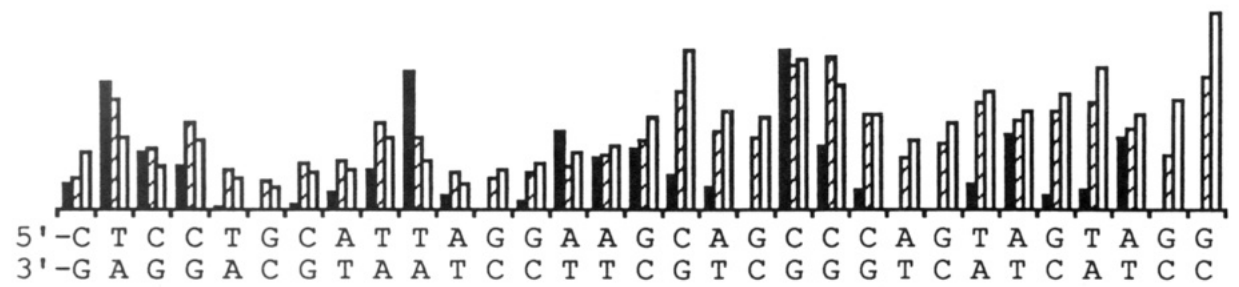

FIGURE 4: Histograms of cutting sites of thiol- and heat-induced DNA cleavage by esperamicin A_1. Blackened, shaded, and unshaded columns represent the DNA cutting of esperamicin A_1 induced by dithiothreitol, 37 °C, and 85 °C, respectively.

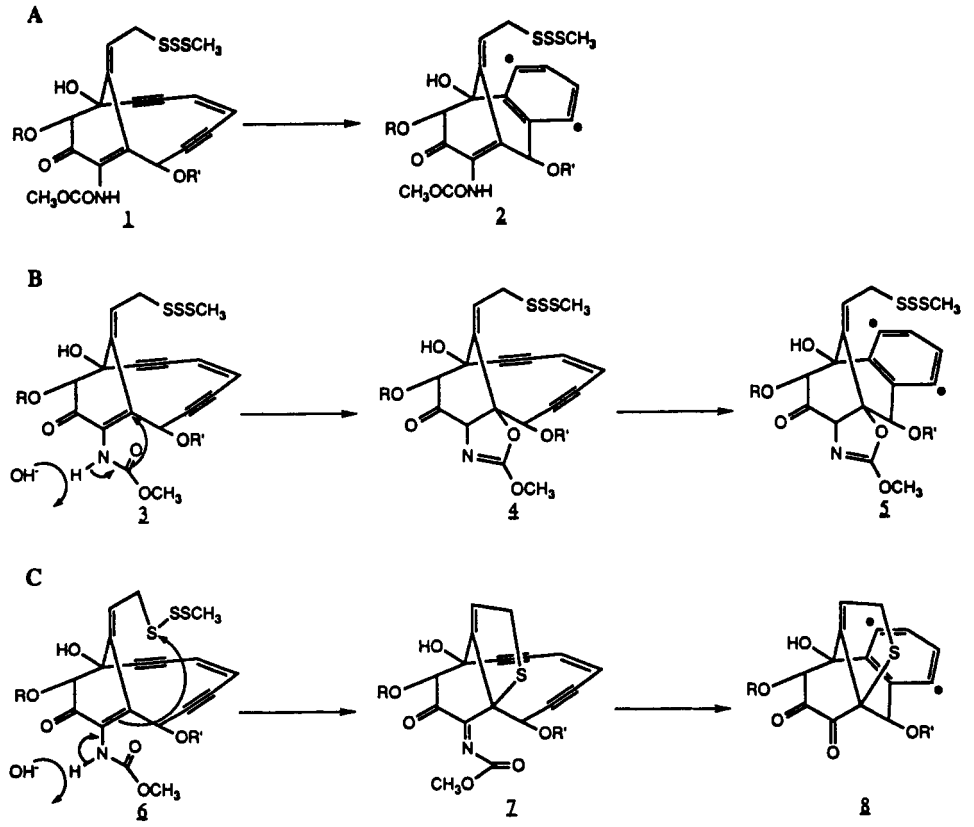

FIGURE 5: A probable mechanism for nonreductive activation of esperamicin A_1.

1990). On the basis of stability to spontaneous cyclization and molecular mechanics calculations, Nicolaou et al. (1988a) determined that the crucial turning point in the distance of the triple bond ends must be in the range of 3.31–3.20 Å at room temperature. The distance of the two triple bonds of the aglycon moiety in esperamicin–calicheamicin antitumor antibiotics is estimated to be 3.36 Å. This distance suggests that the antibiotics stabilize at room temperature because this distance is more extensive than the crucial turning point. At a much higher temperature, however, these drugs may be able to achieve the Bergman's rearrangement as a result of more drastic thermal oscillation of the enediyne (Tomioka et al., 1989; Magnus et al., 1988, 1990; Nagata et al., 1989; Mantlo & Danishefsky, 1989). Indeed, esperamicin A_1 does not indicate potent DNA cutting activity at 20 °C, but it does at 50 °C and also at 37 °C.

The second possibility is the activation of the aglycon moiety with an intramolecular functional group other than the trisulfide portion (Haseltine & Danishefsky, 1989). For example, a $-NHCOOCH_3$ group in the aglycon instead of the trisulfide may function as a trigger. Figure 5B displays a possible mechanism of active-radical formation for the heat-induced breakage of DNA by esperamicin A_1. The compound **5** could arise from esperamicin A_1 by activation of the $-NHCOOCH_3$ group, the Michael's addition to the bridgehead double bond, and aromatization of the enediyne core. If this pathway is real, the reaction will be catalyzed by a hydroxyl anion. Alkaline conditions accelerated the DNA cleavage by esperamicin A_1 at 50 °C. Here, a species such as **2** following hydrogen atom abstraction would be a highly unstable anti Bredt's rule bicyclonon-1-ene and would be expected to undergo a further reaction, e.g., cyclization to yield a product corresponding to the hydrogen atom abstracted product of **5**. Thus, distinguishing between routes A and B might be problematic. On the other hand, in addition to the cyclization mechanism illustrated, a base-catalyzed RAR involving the urethane and the trisulfide (or disulfide) may also be possible as outlined in Figure 5C. The HPLC technique gave a new less polar product on heat activation of esperamicin A_1. We must determine the structure of this product for a reliable argument on its mechanism. Unfortunately, structural assignment of the compound is not fully established at the present stage.

In conclusion, thermotherapeutic temperature is very effective for stimulating DNA nicking by esperamicin A_1. In the heat-induced DNA cleavage of esperamicin antibiotics, the methyl trisulfide group of the aglycon moiety does not function as a trigger of the reaction and the DNA-cutting mode is clearly different from that of the thiol-activated esperamicin A_1. Probably, the action of the heat-activated esperamicin A_1 is due to direct Bergman's rearrangement by high temperature or to the rearrangement by activation of the aglycon with an intramolecular functional group.

Supplementary Material Available

One figure showing HPLC separation of esperamicin A_1 after heating for 18 h (1 page). Ordering information is given on any current masthead page.

Registry No. Esperamicin A_1, 99674-26-7; esperamicin C, 107453-55-4; esperamicin D, 107473-04-1; esperamicin Z, 119341-52-5; esperamicin disulfide, 135598-75-3; calicheamicin γ_1, 108212-75-5.

References

Ellestad, G. A., Hamann, P. R., Zein, N., Morton, G. O., Siegel, M. M., Pastel, M., Borders, D. B., & McGahren, W. J. (1989) *Tetrahedron Lett. 30*, 3033–3036.

Goldberg, I. H. (1987) *Free Radical Biol. Med. 3*, 41–54.

Golik, J., Dubay, G., Groenewold, G., Kawaguchi, H., Konishi, M., Krishnan, B., Ohkuma, H., Saitoh, K., & Doyle, T. W.

(1987) *J. Am. Chem. Soc. 109*, 3461–3464.
Haseltine, J. N., & Danishefsky, S. J. (1989) *J. Am. Chem. Soc. 111*, 7638–7640.
Lee, M. D., Dunne, T. S., Change, C. C., Ellestad, G. A., Siegel, M. M., Morton, G. O., McGahren, W. J., & Borders, D. B. (1987) *J. Am. Chem. Soc. 109*, 3466–3468.
Lockhart, T. P., Comita, P. B., & Bergman, R. G. (1981) *J. Am. Chem. Soc. 103*, 4082–4090.
Long, B. H., Golik, J., Forenza, S., Ward, B., Rehfuss, R., Dabrowiak, J. C., Catino, J. J., Musial, S. T., Brookshire, K. W., & Doyle, T. W. (1989) *Proc. Natl. Acad. Sci. U.S.A. 86*, 2–6.
Magnus, P., Lewis, R. T., & Huffman, J. C. (1988) *J. Am. Chem. Soc. 110*, 6921–6923.
Magnus, P., Fortt, S., Pitterna, T., & Snyder, J. P. (1990) *J. Am. Chem. Soc. 112*, 4986–4987.
Mantlo, N. B., & Danishefsky, S. J. (1989) *J. Org. Chem. 54*, 2781–2783.
Maxam, A. M., & Gilbert, W. (1980) *Methods Enzymol. 65*, 499–560.
Nagata, R., Yamanaka, H., Okazaki, E., & Saito, I. (1989) *Tetrahedron Lett. 30*, 4995–4998.
Nicolaou, K. C., Ogawa, Y., Zuccarello, G., & Kataoka, H. (1988a) *J. Am. Chem. Soc. 110*, 7247–7248.
Nicolaou, K. C., Zuccarello, G., Ogawa, Y., Schweiger, E. J., & Kumazawa, T. (1988b) *J. Am. Chem. Soc. 110*, 4866–4868.
Shiraki, T., & Sugiura, Y. (1990) *Biochemistry 29*, 9795–9798.
Snyder, J. P. (1989) *J. Am. Chem. Soc. 111*, 7630–7632.
Snyder, J. P. (1990) *J. Am. Chem. Soc. 112*, 5367–5369.
Sugiura, Y., Uesawa, Y., Takahashi, Y., Kuwahara, J., Golik, J., & Doyl, T. W. (1989) *Proc. Natl. Acad. Sci. U.S.A. 86*, 7672–7676.
Sugiura, Y., Shiraki, T., Konishi, M., & Oki, T. (1990) *Proc. Natl. Acad. Sci. U.S.A. 87*, 3831–3835.
Tomioka, K., Fujita, H., & Koga, K. (1989) *Tetrahedron Lett. 30*, 851–854.
Uesawa, Y., Kuwahara, J., & Sugiura, Y. (1989) *Biochem. Biophys. Res. Commun. 164*, 903–911.
Zein, N., Sinha, A. M., McGahren, W. J., & Ellestad, G. A. (1988) *Science 240*, 1198–1201.
Zein, N., McGahren, W. J., Morton, G. O., Ashcroft, J., & Ellestad, G. A. (1989) *J. Am. Chem. Soc. 111*, 6888–6890.

Binding of Triple Helix Forming Oligonucleotides to Sites in Gene Promoters†

Ross H. Durland,‡ Donald J. Kessler,‡ Sandy Gunnell,‡ Madeleine Duvic,§ B. M. Pettitt,∥ and Michael E. Hogan*,‡

Center for Biotechnology, Baylor College of Medicine, Woodlands, Texas 77381, Department of Dermatology and Internal Medicine, University of Texas Medical School, Houston, Texas 77030, Department of Chemistry, University of Houston, Houston, Texas 77204-5641

Received May 14, 1991; Revised Manuscript Received July 9, 1991

ABSTRACT: A class of triplex-forming oligodeoxyribonucleotides (TFOs) is described that can bind to naturally occurring sites in duplex DNA at physiological pH in the presence of magnesium. The data are consistent with a structure in which the TFO binds in the major groove of double-stranded DNA to form a three-stranded complex that is superficially similar to previously described triplexes. The distinguishing features of this class of triplex are that TFO binding apparently involves the formation of hydrogen-bonded G·GC and T·AT triplets and the TFO is bound antiparallel with respect to the more purine-rich strand of the underlying duplex. Triplex formation is described for targets in the promoter regions of three different genes: the human c-*myc* and epidermal growth factor receptor genes and the mouse insulin receptor gene. All three sites are relatively GC rich and have a high percentage of purine residues on one strand. DNase I footprinting shows that individual TFOs bind selectively to their target sites at pH 7.4–7.8 in the presence of millimolar concentrations of magnesium. Electrophoretic analysis of triplex formation indicates that specific TFOs bind to their target sites with apparent dissociation constants in the 10^{-7}–10^{-9} M range. Strand orientation of the bound TFOs was confirmed by attaching eosin or an iron-chelating group to one end of the TFO and monitoring the pattern of damage to the bound duplex DNA. Possible hydrogen-bonding patterns and triplex structures are discussed.

Triple-helical nucleic acid structures can be formed from synthetic polymers, as the result of internal disproportionation of polypurine arrays in duplexes, or by the binding of short oligonucleotides to purine-rich duplex DNA segments (Felsenfeld et al., 1957; Felsenfeld & Rich, 1957; Lipsett, 1963, 1964; Howard et al., 1964; Morgan & Wells, 1968; Thiele & Guschlbauer, 1971; Haas & Guschlbauer, 1976; Marck & Thiele, 1978; Lyamichev et al., 1985, 1986, 1988; Moser & Dervan, 1987; Broitman et al., 1987; Kohwi & Kohwi-Shigematsu, 1988; Htun & Dahlberg, 1988; Harvey et al., 1988; Hanvey et al., 1988; Fedorova et al., 1988; Praseuth et al., 1988). Several groups have described and studied homopolymeric DNA triplexes such as poly(dT)·poly(dA)·poly(dT) and poly(dC⁺T)·poly(dGA)·poly(dTC) (Riley et al., 1966; Arnott & Selsing, 1974; Arnott et al., 1976; Lee et al., 1979). More recently, synthetic oligonucleotides composed of C and/or T residues have been shown to form stable triple helices by binding to specific oligopurine regions in double-stranded DNA (Moser & Dervan, 1987; Lyamichev et al., 1988; Fe-

†Supported by grants from the Office of Naval Research and Triplex Pharmaceutical Corporation to M.E.H., from the NIH to M.D. and M.E.H., and from the Texas Advanced Technology Program to M.D. and M.E.H.

‡Baylor College of Medicine.
§University of Texas Medical School.
∥University of Houston.

0006-2960/91/0430-9246$02.50/0